



# OPEN Differences in risk factors associated with the initiation and progression of mitral annular calcification in asymptomatic individuals

Kyung An Kim<sup>1,2,3</sup>, Hae-Ok Jung<sup>1✉</sup>, So-Young Lee<sup>1,3</sup>, Yuran Ahn<sup>3,4</sup>, Mi-Hyang Jung<sup>1,3</sup>, Woo-Baek Chung<sup>1</sup>, Dong-Hyeon Lee<sup>5</sup>, Ho-Joong Youn<sup>1</sup>, Donghee Han<sup>6</sup> & Hyuk-Jae Chang<sup>7</sup>

Mitral annular calcification (MAC) is hypothesized to be a representation of atherosclerosis and is associated with adverse outcomes. However, the pathophysiology and risk factors associated with MAC development are not fully understood. Using the KOREA Initiatives on Coronary Artery (KOICA) registry, 738 asymptomatic individuals who underwent health screening with echocardiography and serial cardiac computed tomography (CT) were included for analysis. MAC was identified on CT, and the severity was quantified using Agatston units (AU). Risk factors associated with prevalent MAC and the rate of MAC progression were identified using multivariable regression models. On initial CT, 52 (7.0%) participants showed prevalent MAC, and in this group the median MAC progression rate was 3.4 AU/year (interquartile range: 0.2–14.7) during a median interscan duration of 36.4 months. Factors associated with prevalent MAC were older age ( $p < 0.001$ ), higher body-mass index ( $p = 0.04$ ), diabetes ( $p < 0.01$ ), higher systolic blood pressure ( $p < 0.01$ ), and higher left atrial volume index ( $p = 0.02$ ). Meanwhile, factors associated with faster MAC progression were initial MAC severity ( $p < 0.001$ ), male sex ( $p < 0.01$ ), and higher serum phosphate ( $p < 0.001$ ). Traditional atherosclerotic risk factors have an important role in the initial process of MAC development. The association between left atrial volume index and prevalent MAC further suggests the implication of elevated left ventricular filling pressure in MAC initiation. Conversely, initial MAC severity and mineral metabolism were found to be major determinants in the later phase of MAC progression.

**Keywords** Mitral annular calcification, Atherosclerosis, Cardiac computed tomography, Calcium-phosphate metabolism

Mitral annular calcification (MAC), a process characterized by mitral annulus fibrosis and calcification, is hypothesized to be a cardiac manifestation of atherosclerosis, which is associated with adverse outcomes including cardiovascular mortality, stroke, mitral valve dysfunction, and arrhythmias<sup>1–3</sup>. Despite its role in cardiovascular disease, the pathophysiology and risk factors associated with MAC are not fully understood. Traditional cardiovascular risk factors, such as old age, obesity, diabetes, hypertension, dyslipidemia, and smoking, have been associated with the development of MAC<sup>1,4</sup>. Conditions leading to increased mitral valve stress, such as aortic stenosis and left ventricular hypertrophy (LVH), have also been implicated<sup>5,6</sup>. However, factors associated with the progression of MAC severity are poorly characterized. Previous studies have noted

<sup>1</sup>Division of Cardiology, Department of Internal Medicine, Seoul St. Mary's Hospital, The Catholic University of Korea, 222 Banpo-daero, Seocho-gu, Seoul 06591, Republic of Korea. <sup>2</sup>Division of Cardiology, Department of Internal Medicine, Incheon St. Mary's Hospital, The Catholic University of Korea, Incheon, Republic of Korea. <sup>3</sup>Catholic Research Institute for Intractable Cardiovascular Disease, College of Medicine, The Catholic University of Korea, Seoul, Republic of Korea. <sup>4</sup>Division of Cardiology, Department of Internal Medicine, Uijeongbu St. Mary's Hospital, The Catholic University of Korea, Uijeongbu, Republic of Korea. <sup>5</sup>Health Promotion Center, Seoul St. Mary's Hospital, The Catholic University of Korea, Seoul, Republic of Korea. <sup>6</sup>Department of Imaging, Cedars-Sinai Medical Center, Los Angeles, CA, USA. <sup>7</sup>Division of Cardiology, Yonsei Cardiovascular Center, Yonsei University Health System, Seoul, Republic of Korea. ✉email: hojheart@gmail.com

baseline MAC severity as the primary predictor of MAC progression, suggesting that while atherosclerotic processes may initiate MAC, they are only modestly associated with its progression<sup>7</sup>. Osteoblast activation and abnormal calcium-phosphate metabolism have been identified as the main drivers in the latter stage of aortic valve calcification<sup>8–10</sup>, proposing a similar mechanism for MAC<sup>11</sup>. Therefore, in this study, we aimed to identify factors associated with MAC initiation and progression using multimodality imaging in subjects undergoing serial cardiac computed tomography (CT) and echocardiography for self-referred health examination.

## Patients and methods

### Study design and population

We used data collected from the KOrea Initiatives on Coronary Artery calcification (KOICA) registry, which has been detailed in previous reports<sup>12,13</sup>. Briefly, the KOICA registry is an observational, retrospective, multicenter registry consisting data of individuals who underwent cardiac CT for coronary artery calcium scoring as part of their self-referred health examination, which was performed at six healthcare centers in Korea. From the registry, we further selected subjects who underwent examination at Seoul St. Mary's Hospital (data collected between April 2009 and July 2016), since in our healthcare center, cardiac CT scans are obtained as part of a cardiovascular-focused program including echocardiography, and thus same-day echocardiograms were available for analysis. The final study was done on the participants with at least two cardiac CT scans during the duration of follow-up. All CT scans, including the repeat examinations, were obtained during self-referred health examination and were taken at the healthcare center. During the health examination, demographic factors and medical history were collected using a detailed, self-reported questionnaire. As the subjects underwent testing as part of a general health examination, the possibility of symptomatic patients being included was low, and medical records were reviewed to ensure that no participants had symptoms related to cardiovascular disease or previous radiation therapy at the time of initial or repeat CT scanning. Laboratory samples were obtained on the same day as the CT scan after a 12-hour fast, and the lipid profile including low-density lipoprotein cholesterol levels were measured using an automatic analyzer by a direct enzymatic method (7600 – 210; Hitachi Medical Corp., Tokyo, Japan). The estimated glomerular filtration function (eGFR) was calculated using the CKD-EPI equation, and chronic kidney disease (CKD) was defined as either an eGFR < 60 mL/min/1.73 m<sup>2</sup> or a self-reported history of CKD. The study was approved by the institutional review board of Seoul St. Mary's Hospital (IRB KC23RIS10357), which waived the need for written informed consent due to the retrospective nature of the study. This study complies with the principles of the 1975 Declaration of Helsinki.

### Data acquisition

As described in previous studies, cardiac CT scans at our center were obtained using a 64-slice, dual-source CT scanner (SOMATOM Definition, Siemens, Forchheim, Germany)<sup>14</sup>. Prior to contrast administration, a non-contrast, prospectively triggered calcium scan at 70% of the RR interval was performed (tube voltage 120 kVp, 0.6-mm slice collimation, gantry rotation time 330 ms, maximum tube current 400 mAs, with adjustment for body size as necessary). Following this, 80–110 mL of iodinated contrast was administered, and a retrospective electrocardiogram-gated scanning protocol was applied to obtain enhanced CT angiography scans. All cardiac CT scans were reconstructed using a three-dimensional workstation (Advantage Windows Workstation 4.3, GE Healthcare, Milwaukee, Wisconsin, USA) with 3 mm slice thickness.

The severity of MAC was quantitatively assessed using a commercially available CT processing program (3 mensio Structural Heart 9.0, Pie Medical Imaging, Maastricht, The Netherlands) using the method described by Agatston et al. as in previous studies<sup>7,15,16</sup>. The software automatically detects pixels with values  $\geq 130$  Hounsfield Units and reports values for the sum of each contiguous area in Agatston units (AU). Each calcified lesion on the mitral annulus was carefully selected, excluding calcifications found in the coronary arteries, aortic valve, and left ventricular outflow tract. The MAC score, defined as the sum of the values for each lesion, was assessed by two cardiologists (K.A.K. and S.-Y.L.) with 3 years of experience in cardiac imaging. Lesions with MAC score > 0 were independently scored by both investigators, and the interobserver agreement was assessed using Bland-Altman and scatter plots. In cases of uncertainty, a third cardiologist (H.-O.J.) with more than 20 years of cardiac imaging experience was consulted.

Transthoracic echocardiography was performed by trained sonographers following standard guidelines under the supervision of cardiologists specializing in cardiac imaging (D.-H.L., W.-B.C., H.-O.J., and H.-J.Y.)<sup>17</sup>. Commercially available ultrasound machines with 2.5- to 3.5-MHz transducers (GE Vivid E7 and Vivid E9, Chicago, Illinois, USA; Philips iE33, Amsterdam, the Netherlands) were used. Only the initial echocardiograms were selected for analysis. Since MAC is known to disproportionately affect the early diastolic mitral annular velocity ( $e'$ ) of the lateral wall, only the septal mitral annular velocity was used for evaluating diastolic function, with septal  $E/e' > 15$  indicating elevated left ventricular filling pressure (LVFP)<sup>17,18</sup>.

### Statistical analysis

Categorical data are presented as numbers and frequencies and compared using the  $\chi^2$  test or Fisher's exact test. Continuous variables are expressed as mean  $\pm$  standard deviation or median [interquartile range (IQR)], depending on variable distribution, and compared using the Student's *t*-test or Mann-Whitney *U* test as appropriate.

Prevalent MAC was defined as detectable MAC (MAC score > 0 AU) on initial CT. Factors associated with prevalent MAC were identified using logistic regression. Variables with  $p < 0.25$  on univariable analysis were entered into multivariable analysis, and the stepwise Akaike information criterion method was utilized to select the final variables. For each significant predictor, the optimal cut-off value was determined by the point on the receiver operating characteristic curve maximizing the Youden index. Restricted cubic splines were also

constructed with the optimal cut-off values as the reference point, with knots placed at the 5th, 35th, 65th, and 95th percentiles to visualize the relationship between each significant variable and the probability of MAC initiation.

The MAC progression rate was defined as the annualized absolute difference in MAC scores between the first and last CT scans for the participants with prevalent MAC on the first CT scan, as described in previous studies<sup>7</sup>. The relationship between MAC progression rate and the risk factors was assessed using linear regression of ordinary least squares. Variables with  $p < 0.25$  on univariable analysis were entered into multivariable analysis, and the stepwise Akaike information criterion method was utilized to select the final variables. eGFR was included in the analysis to adjust for the presence of serum calcium and phosphate levels in the model. Collinearity was assessed using the variance inflation factor (VIF), which was  $< 5$  for each variable in the final model. Homoskedasticity was also assessed and satisfied using White's test and by plots of the residuals and fitted values. As a sensitivity analysis and to minimize the influence of outliers, the analysis was repeated using robust linear regression with standard M-regression estimates and also with square-root transformed MAC scores. Finally, since measurements of cardiac calcification are subject to interscan variability, MAC progression was also analyzed as a binary variable using logistic regression, wherein MAC progression was defined as  $\sqrt{(\text{follow-up MAC score}) - (\text{baseline MAC score})} > 2.5$ , in order to minimize the effect of changes from interscan variability, and as used in studies on coronary artery calcification<sup>19</sup>.

Statistical analyses were performed using R Statistical Software version 4.3.1 (R Foundation for Statistical Computing, Vienna, Austria) and SPSS version 26.0 (IBM, Armonk, New York, USA), and a two-sided  $p$ -value  $< 0.05$  was considered statistically significant.

## Results

### Baseline characteristics

From a total of 93,914 individuals enrolled in the KOICA registry, we selected 6,641 participants who underwent examination at Seoul St. Mary's Hospital. After the exclusion of two individuals with missing data, 738 subjects with at least two CT scans were included in the final study (Fig. 1). The median duration between the first and last CT scans was 36.4 (IQR: 23.5–50.3) months. On initial CT examination, 52 (7.0%) individuals had prevalent MAC, with a median MAC score of 11.8 (IQR: 2.3–69.0) AU. Regarding the location of MAC, the anterior mitral annulus was involved in 13 (25.0%) individuals, the posterior mitral annulus in 42 (80.8%) individuals, and both annuli in 3 (5.8%) participants. The distribution of MAC scores was highly skewed to the right, and the majority of lesions had a low MAC score (Supplementary Figure S1A). On the last CT assessment, the MAC score of patients with prevalent MAC increased to a median of 25.0 (IQR: 5.6–93.8) AU, with a median progression rate of 3.4 (IQR: 0.2–14.7) AU/year (Supplementary Figure S1B). The interobserver agreement of the MAC score was excellent with an intraclass correlation coefficient of 0.999 (Supplementary Figure S2).

The baseline characteristics of the study population are shown in Table 1. The median age was 57 years, and 80.6% were male. The proportion of participants with major co-morbidities was low overall. On echocardiography, only one had moderate mitral regurgitation, and none had significant mitral stenosis or findings indicative of an increased transmitral pressure gradient (e.g., increased turbulent flow by color Doppler imaging across the mitral valve). Compared to the individuals without MAC, those with prevalent MAC were older; had a higher body-mass index (BMI); were more likely to have hypertension, diabetes, or dyslipidemia; presented with higher systolic and diastolic blood pressures; had higher HbA1c and fasting glucose levels; and had lower eGFR and more coronary artery calcification. On echocardiography, participants with prevalent MAC had a higher left ventricular mass index (LVMI), larger LAVI, lower septal  $e'$  velocities, higher  $E/e'$  values, and higher peak tricuspid regurgitation velocities.

### Risk factors for prevalent mitral annular calcification

On univariable analysis, older age, higher BMI, diabetes, hypertension, dyslipidemia on lipid-lowering medications, higher systolic blood pressure (SBP), higher HbA1c, lower eGFR, higher LVMI, higher LAVI, higher  $E/e'$ , and higher peak tricuspid regurgitation velocity were associated with prevalent MAC (Table 2). After multivariable adjustment, old age (odds ratio [OR] per 10 years 1.07, 95% confidence interval [CI] 1.05–1.09,  $p < 0.001$ ), higher BMI (OR per 5 kg/m<sup>2</sup> 1.03, 95% CI 1.00–1.06,  $p = 0.04$ ), diabetes (OR 1.08, 95% CI 1.02–1.14,  $p < 0.01$ ), higher SBP (OR per 1 mmHg 1.02, 95% CI 1.01–1.04,  $p < 0.01$ ), and higher LAVI (OR per 5 ml/m<sup>2</sup> 1.02, 95% CI 1.01–1.03,  $p = 0.02$ ) emerged as independent predictors of MAC initiation (Model 1). The individual optimal cut-off points for predicting prevalent MAC were age  $> 63$  years, BMI  $> 25.6$  kg/m<sup>2</sup>, SBP  $> 134$  mmHg, and LAVI  $> 28.2$  ml/m<sup>2</sup> (Supplementary Figure S3). The C-statistic value of the multivariable logistic regression model was 0.83, demonstrating adequate discriminative power. To further investigate the findings suggesting an association between diastolic dysfunction and MAC, an additional analysis substituting LAVI in the multivariable regression model with septal  $E/e'$  was performed, and septal  $E/e' > 15$  was also found to be associated with prevalent MAC (OR 1.20, 95% CI 1.04–1.38,  $p = 0.02$ ) (Supplementary Table S1). Restricted cubic spline curves also showed a positive correlation between each variable and the probability of MAC (Fig. 2).

### Risk factors for the progression rate of mitral annular calcification

On unadjusted linear regression, initial MAC severity and serum calcium levels were the only significant predictors of a higher MAC progression rate (measured in AU/year) (Table 3). After multivariable adjustment, initial MAC severity (regression coefficient per 1 AU 0.22, 95% CI 0.17–0.27,  $p < 0.001$ ), male sex (regression coefficient 22.22, 95% CI 6.75–37.70,  $p < 0.01$ ), and phosphate (regression coefficient per 1 mg/dL 28.85, 95% CI 14.02–43.67,  $p < 0.001$ ) emerged as independent factors of MAC progression rate, whereas higher LVMI approached, but did not reach, statistical significance (multiple  $R^2 = 0.742$ , F-test  $p < 0.001$ ). Notably, the

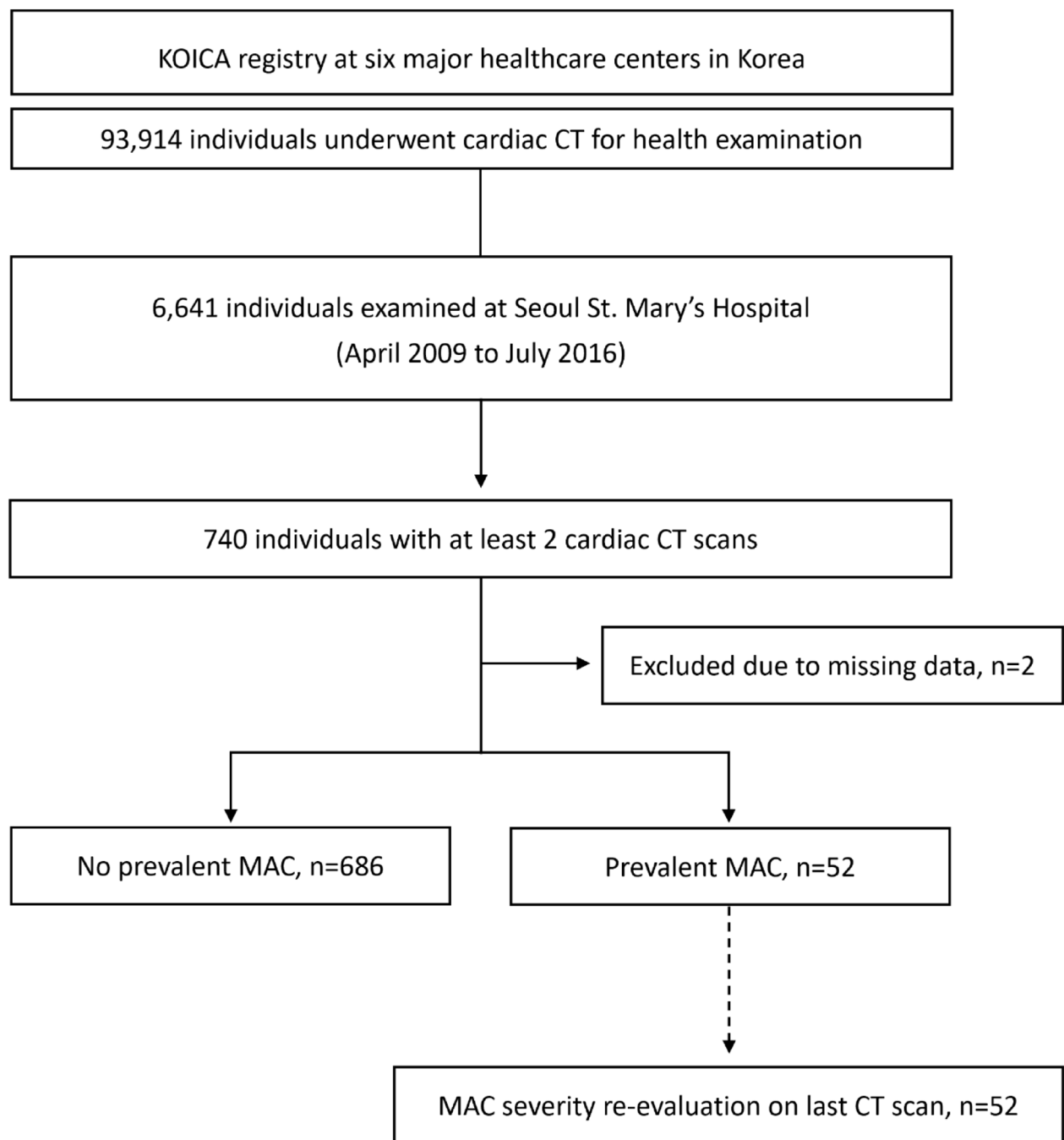


**Fig. 1.** Selection process of the study population. KOICA, Korea Initiatives on Coronary Artery calcification; CT, computed tomography; MAC, mitral annular calcification.

association between serum calcium and MAC progression lost significance in the multivariable analysis. The relationship between the MAC progression rate and initial MAC severity and phosphate levels are shown in **Supplementary Figure S4**.

Sensitivity analysis using robust linear regression also found that initial MAC severity (regression coefficient per 1 AU 0.11, 95% CI 0.07–0.15,  $p < 0.001$ ) and phosphate (regression coefficient per 1 mg/dL 6.20, 95% CI 1.30–11.02,  $p = 0.01$ ) were independent predictors of a higher rate of MAC progression, whereas a history of hypertension approached, but did not reach, statistical significance (multiple  $R^2 = 0.735$ ) (**Supplementary Table S2**). An additional sensitivity analysis using square-root transformed MAC scores yielded similar results, indicating initial MAC severity, male sex, phosphate, and LVMI as significant predictors of a higher MAC progression rate (**Supplementary Table S3**). When MAC progression was analyzed as a binary variable, 19 (36.5%) participants with initial MAC met the criteria for progression, and initial MAC severity, phosphate, and LVMI were significant predictors of MAC progression (**Supplementary Table S4**).

Characteristics	No MAC ( <i>n</i> = 686)	MAC ( <i>n</i> = 52)	<i>p</i> -value
Age (year)	54 [49–59]	64 [57–70]	< 0.001
Male (%)	555 (80.9)	40 (76.9)	0.60
BMI (kg/m <sup>2</sup> )	24.5 [22.8–26.3]	25.4 [24.4–27.0]	0.01
Smoking	279 (40.7)	13 (25.0)	0.04
Diabetes (%)	83 (12.1)	16 (30.8)	< 0.001
on medication (%)	74 (10.8)	16 (30.8)	< 0.001
Hypertension (%)	229 (33.4)	25 (48.1)	0.03
on medication (%)	202 (29.4)	25 (48.1)	0.01
Dyslipidemia (%)	122 (17.8)	13 (25.0)	0.19
on medication (%)	81 (11.8)	13 (25.0)	0.01
Previous PCI (%)	52 (7.6)	4 (7.7)	0.09
Atrial fibrillation (%)	3 (0.4)	1 (2.0)	0.25
CKD (%)	2 (0.3)	0 (0.0)	1.00
Stroke (%)	7 (1.0)	2 (3.8)	0.26
SBP (mmHg)	124 [115–132]	131 [126–138]	< 0.001
DBP (mmHg)	75.1 ± 9.3	77.8 ± 8.1	0.04
HR (beats/min)	63 [57–69]	62 [57–66]	0.21
WBC (10 <sup>9</sup> /L)	5.5 [4.6–6.7]	5.9 [4.6–6.8]	0.53
Hemoglobin (mg/dL)	15.0 ± 1.4	15.0 ± 1.5	0.89
HbA1c (%)	5.6 [5.4–5.9]	5.8 [5.6–6.4]	< 0.01
Glucose (mg/dL)	99 [91–111]	107 [97–132]	< 0.01
LDL-C (mg/dL)	118 [100–142]	108 [86–134]	0.06
Triglycerides (mg/dL)	108 [73–162]	97 [77–144]	0.47
eGFR (mL/min/1.73 m <sup>2</sup> )	84.6 [78.0–91.4]	78.4 [72.5–86.2]	< 0.001
Calcium (mg/dL)	9.2 [8.9–9.4]	9.2 [9.0–9.4]	0.98
Phosphate (mg/dL)	3.4 [3.1–3.7]	3.4 [3.2–3.8]	0.68
hs-CRP (mg/dL)	0.07 [0.03–0.14]	0.06 [0.03–0.14]	0.81
CAC score (AU) <sup>a</sup>	0.0 [0.0–28.8]	178.0 [12.1–502.9]	< 0.001
LVEF (%)	66.0 [62.7–69.3]	64.2 [61.5–69.0]	0.26
LVEDV (mL)	79.0 [66.1–92.2]	81.6 [65.0–90.0]	0.96
LVMI (kg/m <sup>2</sup> )	84.0 [74.4–94.7]	93.0 [81.3–110.8]	< 0.01
LAVI (mL/m <sup>2</sup> )	23.5 [19.9–27.9]	27.0 [23.2–36.1]	< 0.001
E wave velocity (cm/s)	58.5 [50.8–67.7]	60.0 [51.4–65.6]	0.74
Septal e' (cm/s)	6.9 [5.8–8.3]	6.0 [4.8–7.2]	< 0.001
Septal s' (cm/s)	7.6 [6.9–8.5]	7.3 [6.1–8.8]	0.35
Septal E/e'	8.6 [7.3–9.9]	9.9 [8.0–11.9]	< 0.001
>15 (%)	8 (1.3)	4 (7.8)	< 0.01
MR severity			0.66
none/trivial (%)	529 (86.3)	41 (78.8)	
mild (%)	83 (13.5)	11 (21.2)	
> moderate (%)	1 (0.2)	0 (0.0)	
TR V <sub>max</sub> (m/s)	2.2 [2.0–2.3]	2.3 [2.1–2.4]	< 0.01

**Table 1.** Baseline characteristics of the study population stratified according to the presence of mitral annular calcification. a. For those without previous percutaneous coronary intervention. MAC, mitral annular calcification; BMI, body-mass index; PCI, percutaneous coronary intervention; CKD, chronic kidney disease; SBP, systolic blood pressure; DBP, diastolic blood pressure; HR, heart rate; WBC, white blood cell; HbA1c, glycated hemoglobin; LDL-C, low-density lipoprotein cholesterol; eGFR, estimated glomerular filtration rate; hs-CRP, high-sensitivity C-reactive protein; CAC, coronary artery calcification; AU, Agatston units; LVEF, left ventricular ejection fraction; LVEDV, left ventricular end diastolic volume; LVESV, left ventricular end systolic volume; LVMI, left ventricular mass index; RMT, relative wall thickness; LAVI, left atrial volume index; MR, mitral regurgitation; TR V<sub>max</sub>, peak tricuspid regurgitation velocity.

## Discussion

In this study, we assessed MAC using multimodality imaging in a retrospective cohort study of asymptomatic individuals undergoing cardiac CT and echocardiography as part of their self-referred health examination. The prevalence of MAC was 7.0% on the initial CT, and the median progression rate was 3.4 AU/year. Factors

Characteristics	Unadjusted		Multivariable adjusted <sup>a</sup>	
	OR (95% CI)	p-value	OR (95% CI)	p-value
Age (per 10 years)	1.09 (1.06–1.012)	< 0.001	1.07 (1.05–1.09)	< 0.001
Sex				
Male	0.99 (0.95–1.04)	0.74	0.97 (0.93–1.02)	0.21
Female	referent		referent	
BMI (per 5 kg/m <sup>2</sup> )	1.04 (1.01–1.06)	0.03	1.03 (1.00–1.06)	0.04
Smoking	0.99 (0.96–1.01)	0.24		
Diabetes	1.11 (1.05–1.17)	< 0.001	1.08 (1.02–1.14)	< 0.01
Hypertension	1.07 (1.03–1.11)	< 0.01		
Dyslipidemia	1.10 (0.96–1.06)	0.71		
Glucose-lowering medications	1.12 (1.06–1.18)	< 0.001		
Antihypertensive medications	1.06 (1.02–1.10)	< 0.01		
Lipid-lowering medications	1.07 (1.01–1.13)	0.02		
SBP (per 10 mmHg)	1.06 (1.04–1.08)	< 0.001	1.02 (1.01–1.04)	< 0.01
DBP (per 10 mmHg)	1.00 (0.98–1.02)	0.98		
HR (per 10 beats/min)	0.99 (0.97–1.01)	0.37		
WBC count (per 10 <sup>9</sup> /L)	1.01 (0.99–1.02)	0.32		
HbA1c (per 1%)	1.04 (1.01–1.07)	< 0.01		
LDL-C (per 10 mg/dL)	0.99 (0.98–1.00)	0.05		
Triglycerides (per 10 mg/dL)	1.00 (0.99–1.01)	0.29		
eGFR (per 10 mL/min/1.73 m <sup>2</sup> )	0.96 (0.95–0.98)	< 0.001		
Calcium (per 1 mg/dL)	1.00 (0.95–1.06)	0.95		
Phosphate (per 1 mg/dL)	1.01 (0.97–1.05)	0.53		
hs-CRP (per 1 mg/dL)	1.01 (0.95–1.08)	0.71		
LVEF (per 10%)	0.98 (0.95–1.02)	0.37		
LVEDV (per 10 ml)	1.00 (0.99–1.01)	0.58		
LVMI (per 10 g/m <sup>2</sup> )	1.02 (1.01–1.04)	< 0.001		
LAVI (per 5 ml/m <sup>2</sup> )	1.06 (1.03–1.09)	< 0.001	1.02 (1.01–1.03)	0.02
MR severity				
none/trivial	referent			
mild/moderate/severe	1.02 (0.97–1.08)	0.45		
Septal E/e' (per 1)	1.02 (1.01–1.03)	< 0.001		
Septal E/e' > 15	1.31 (1.13–1.51)	< 0.001		
TR V <sub>max</sub> (per 1 m/s)	1.12 (1.02–1.23)	0.02		

**Table 2.** Identification of risk factors for prevalent mitral annular calcification. a. Adjusted for age, sex, body-mass index, diabetes, systolic blood pressure, and left atrial volume index. OR, odds ratio; CI, confidence interval; BMI, body-mass index; SBP, systolic blood pressure; HR, heart rate; WBC, white blood cell; HbA1c, glycated hemoglobin; LDL-C, low-density lipoprotein cholesterol; eGFR, estimated glomerular filtration rate; hs-CRP, high-sensitivity C-reactive protein; LVEF, left ventricular ejection fraction; LVEDV, left ventricular end diastolic volume; LVMI, left ventricular mass index; LAVI, left atrial volume index; MR, mitral regurgitation; TR V<sub>max</sub>, peak tricuspid regurgitation velocity.

associated with prevalent MAC included older age, higher BMI, diabetes, higher SBP, and higher LAVI, whereas factors associated with a higher MAC progression rate included severe initial MAC, male sex, and higher serum phosphate.

Previous studies have shown that traditional atherosclerotic risk factors, such as old age, obesity, diabetes, hypertension, dyslipidemia, and smoking, are associated with the presence of MAC<sup>4,5,7</sup>. Hemodynamic factors leading to increased stress on the mitral valve apparatus are also likely to have a role in MAC development<sup>5,11,20</sup>. Our results are in agreement with previous studies in identifying the established atherosclerotic risk factors of old age, obesity, diabetes, and hypertension as risk factors for prevalent MAC. Moreover, since LAVI is reflective of LVFP and mean left atrial pressure<sup>21,22</sup>, its association with MAC further supports the role of hemodynamic stress in MAC development. Other echocardiographic parameters indicating elevated LVFP were significant in univariable analysis but superseded by LAVI in the final multivariable model, and substitution for LAVI with septal E/e' yielded similar conclusions. Our study also shows the utility of multimodality imaging in MAC assessment, as in addition to ascertaining the presence of mitral valve dysfunction due to MAC, echocardiography can comprehensively assess hemodynamics and cardiac function, while CT has superior sensitivity in MAC detection and can perform objective quantification of lesion severity<sup>23</sup>. However, we acknowledge that there is



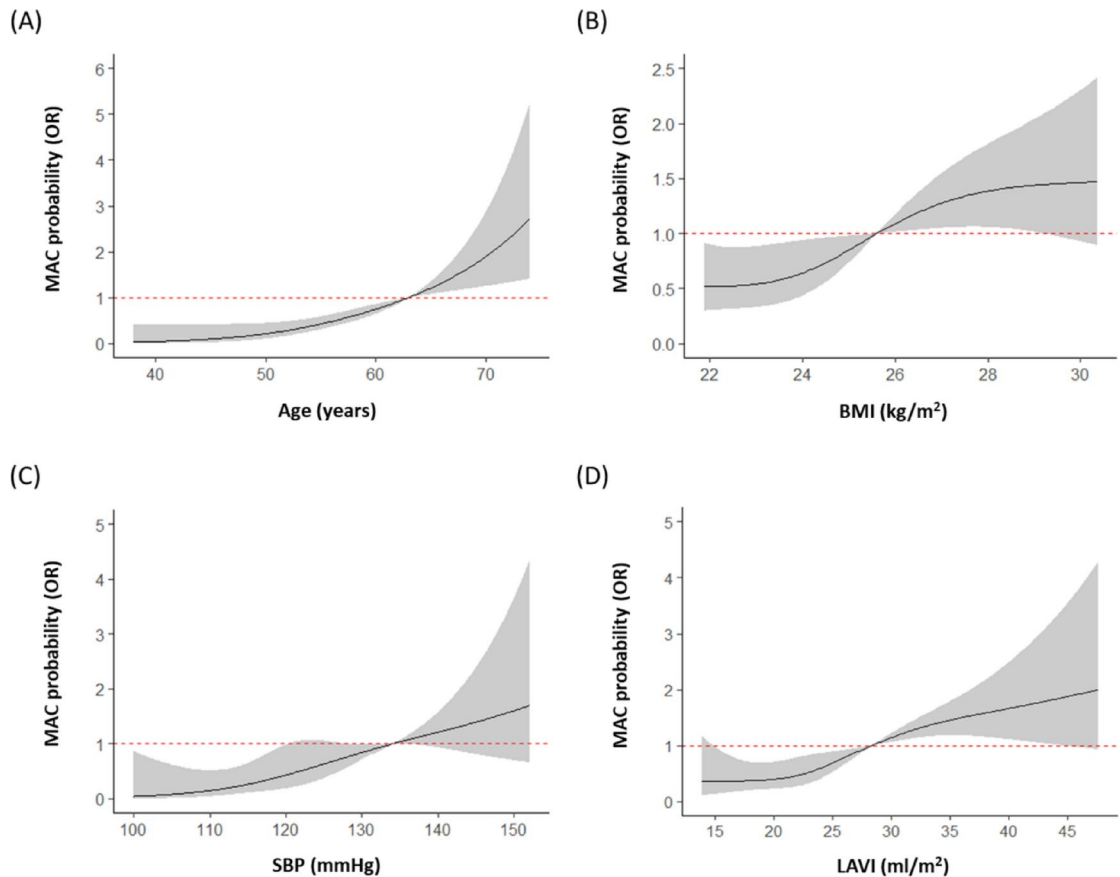


**Fig. 2.** Restricted cubic splines demonstrating the relationship between the probability of mitral annular calcification (A) age (B) body-mass index (C) systolic blood pressure (D) left atrial volume index. The reference values for each variable were determined using the optimal cut-off points for receiver operating characteristic curves (Figure S4). Adjustments were made for age, body-mass index, diabetes, systolic blood pressure, and left atrial volume index. MAC, mitral annular calcification; OR, odds ratio; BMI, body-mass index; SBP, systolic blood pressure; HbA1c, glycated hemoglobin; LAVI, left atrial volume index.

a possibility that the higher LAVI values associated with MAC may reflect another distinct pathophysiologic process. Further studies will be needed to confirm and determine the mechanisms behind this association.

The differences in the risk factors associated with MAC initiation and the rate of MAC progression, observed not only in our analysis but also in previous studies, suggest a different pathophysiologic process behind each stage of MAC development<sup>7,11,24</sup>. Most of the current evidence on cardiac valve calcification come from studies on aortic valve calcification (AVC) where two distinct phases can be identified: an initiation phase of endothelial damage from increased mechanical stress with a resulting atherosclerotic process of lipid infiltration and inflammation, and a later progression phase of self-perpetuating calcification wherein factors related to osteogenesis and calcium-phosphate metabolism are dominant<sup>9</sup>. A similar mechanism has been proposed for the pathogenesis of MAC, although the extent to which MAC shares similarities with AVC remains unclear<sup>11</sup>. Previous studies have found that traditional atherosclerotic risk factors did not affect MAC progression, indicating baseline MAC severity as the only predominant predictor<sup>7,24</sup>. In the present study, factors associated with a higher MAC progression rate included initial MAC severity, male sex, and phosphate, while the atherosclerotic risk factors that predicted prevalent MAC did not affect its progression, which is consistent with the two-step hypothesis of MAC development.

Notably, higher serum phosphate within the normal range was found to be an independent risk factor for MAC progression even after adjustment for serum calcium and eGFR, demonstrating the role of bone-mineral metabolism in the latter phase of MAC development. The central role of calcium-phosphate metabolism in cardiovascular calcification is supported by data from both preclinical models and cohort studies<sup>10,25–28</sup>. Osteoblast-like activity and calcium-phosphate deposition have been found in histopathologic examination of MAC as well as AVC<sup>8,29</sup>. Higher serum phosphate levels within the normal range were also associated with prevalent AVC and MAC in the Cardiovascular Health Study and with prevalent AVC in the MESA cohort<sup>10,28</sup>. Additionally, phosphate modulates fibroblast growth factor 23 and fetuin-A, which are important regulators of bone-mineral metabolism and have been correlated with MAC development<sup>30,31</sup>. Our findings are therefore consistent with previous studies in demonstrating the role of calcium-phosphate metabolism in MAC development, and further show that it is specifically associated with during the progression phase of MAC.

Characteristics	Unadjusted		Multivariable adjusted <sup>a</sup>	
	Regression coefficient (95% CI)	p-value	Regression coefficient (95% CI)	p-value
Initial MAC severity (per 1 AU)	0.22 (0.17–0.27)	< 0.001	0.22 (0.17–0.27)	< 0.001
Age (per 10 years)	0.15 (–13.09–13.40)	0.98		
Sex				
Male	15.90 (–10.89–42.69)	0.24	22.22 (6.75–37.70)	< 0.01
Female	referent		referent	
BMI (per 5 kg/m <sup>2</sup> )	14.40 (–8.91–37.71)	0.22	10.85 (–3.01–24.74)	0.12
Smoking	6.82 (–19.55–33.18)	0.61		
Diabetes	–4.21 (–28.98–20.56)	0.73		
Hypertension	2.15 (–21.19–25.49)	0.85		
Dyslipidemia	1.63 (–24.80–28.06)	0.90		
Glucose-lowering medications	3.26 (–21.52–28.05)	0.79		
Antihypertensive medications	2.15 (–21.19–25.49)	0.85		
Lipid-lowering medications	1.63 (–24.08–28.06)	0.90		
SBP (per 10 mmHg)	–1.62 (–11.53–8.30)	0.74		
DBP (per 10 mmHg)	–2.41 (–16.96–12.13)	0.74		
HR (per 10 beats/min)	11.72 (–4.36–27.80)	0.15		
WBC count (per 10 <sup>9</sup> /L)	5.18 (–19.43–12.31)	0.15		
HbA1c (per 1%)	3.01 (–13.15–19.17)	0.71		
LDL-C (per 10 mg/dL)	–0.01 (–0.36–0.34)	0.95		
Triglycerides (per 10 mg/dL)	–0.01 (–0.23–0.22)	0.97		
eGFR (per 10 mL/min/1.73 m <sup>2</sup> )	2.49 (–9.88–44.87)	0.69	0.88 (–6.42–8.17)	0.81
Calcium (per 1 mg/dL)	34.75 (4.78–64.72)	0.02	7.14 (–12.60–26.89)	0.47
Phosphate (per 1 mg/dL)	22.67 (–1.47–46.81)	0.07	28.85 (14.02–43.67)	< 0.001
hs-CRP (per 1 mg/dL)	–12.82 (–52.10–26.46)	0.51		
LVEF (per 10%)	–0.49 (–23.22–22.23)	0.97		
LVEDV (per 10 ml)	–1.77 (–6.86–3.11)	0.49		
LVMI (per 10 g/m <sup>2</sup> )	4.53 (–0.72–9.77)	0.09	2.80 (–0.23–5.83)	0.07
LAVI (per 5 ml/m <sup>2</sup> )	1.01 (–6.84–8.84)	0.80		
MR severity		0.74		
none/trivial	referent			
mild/moderate/severe	4.28 (–21.44–29.99)			
MAC location		0.14		
anterior & both	–20.88 (–48.91–7.14)			
posterior	referent			
Septal E/e' (per 1)	0.10 (–3.93–4.14)	0.96		
Septal E/e' > 15	–44.56–43.46	0.98		
TR V <sub>max</sub> (per 1 m/s)	9.52 (–55.14–74.18)	0.77		

**Table 3.** Linear regression for the rate of mitral annular calcification progression in individuals with prevalent mitral annular calcification. a. Adjusted for initial mitral annular calcification severity, sex, body-mass index, estimated glomerular filtration rate, calcium, phosphate, and left ventricular mass index. SBP, systolic blood pressure; HR, heart rate; WBC, white blood cell; HbA1c, glycated hemoglobin; LDL-C, low-density lipoprotein cholesterol; Cr, creatinine; eGFR, estimated glomerular filtration rate; hs-CRP, high-sensitivity C-reactive protein; LVEF, left ventricular ejection fraction; LVEDV, left ventricular end diastolic volume; LVMI, left ventricular mass index; LAVI, left atrial volume index; MR, mitral regurgitation, TR V<sub>max</sub>, peak tricuspid regurgitation velocity.

Previous studies on patients with chronic kidney disease have found that cardiovascular calcifications can regress after the correction of calcium-phosphate metabolism<sup>32,33</sup>, and it is conceivable that a similar process may occur in the general population. Further research will be needed to elucidate the mechanism through which phosphate affects MAC development, and ultimately to identify potential therapeutic targets for slowing MAC progression.

In contrast to the well-documented association between female sex and MAC<sup>1,4,7,11,24,34</sup>, our analysis found that MAC progression was faster in males than in females. The low proportion of females in our cohort and the limited number of participants available for analysis on MAC progression suggest that these results may have been due to chance, and further studies will be needed to confirm these findings.



## Limitations

Despite the findings of our study, several limitations were noted. First, the MAC severity in our study population was generally low, and no participant presented with mitral valve dysfunction that could definitely be attributed to MAC. However, this can be seen as a strength of the study, as it shows that the progression phase starts relatively early in MAC development before hemodynamic derangements become evident. Second, the lower risk of atherosclerosis associated with the East Asian population underscores the need for further studies to assess these findings in other ethnic groups<sup>4,7,12</sup>. Third, due to the small cohort, there were insufficient individuals with new-onset MAC during the follow-up period for analysis, and the number of participants with initial MAC available for analysis on the MAC progression rate was also limited. In addition, the skewed distribution of the MAC scores means the effect of outliers may have influenced the linear regression results. Nevertheless, sensitivity with robust linear regression and square-root transformed MAC scores showed similar conclusions. Fourth, analysis was performed on patient characteristics assessed at baseline, and changes in the status of these risk factors during the follow-up period were not included. Fifth, the study population was comprised of individuals who self-referred for health examinations, which means their characteristics may not fully represent those of the general population. Lastly, given its retrospective nature, there was heterogeneity in patient characteristics and follow-up duration. Although we used multivariable regression to adjust for confounders, we cannot exclude the possibility of remaining bias.

## Conclusion

In a cohort study of asymptomatic individuals undergoing health examination, we assessed MAC through multimodality imaging using cardiac CT and echocardiography. On analysis, different risk factors were associated with prevalent MAC and the rate of MAC progression. Older age, higher BMI, diabetes, higher SBP, and higher LAVI were associated with prevalent MAC, whereas initial MAC severity, male sex, and higher serum phosphate were associated with a higher MAC progression rate. Our results are consistent with the two-step model of valve calcification, and further emphasizes the role of phosphate and bone-mineral metabolism in MAC progression. Further research will be needed to confirm these results and ultimately to identify potential therapeutic targets for slowing MAC progression.

## Data availability

Data are available on reasonable request from the corresponding author.

Received: 30 July 2024; Accepted: 5 May 2025

Published online: 13 May 2025

## References

1. Abramowitz, Y., Jilalawi, H., Chakravarty, T., Mack, M. J. & Makkar, R. R. Mitral annulus calcification. *J. Am. Coll. Cardiol.* **66**, 1934–1941. <https://doi.org/10.1016/j.jacc.2015.08.872> (2015).
2. Fox, C. S. et al. Mitral annular calcification predicts cardiovascular morbidity and mortality: the Framingham heart study. *Circulation* **107**, 1492–1496. <https://doi.org/10.1161/01.cir.0000058168.26163.bc> (2003).
3. O'Neal, W. T. et al. Mitral annular calcification and incident atrial fibrillation in the Multi-Ethnic study of atherosclerosis. *Europace* **17**, 358–363. <https://doi.org/10.1093/europace/euu265> (2015).
4. Kanjanathai, S. et al. Relationships of mitral annular calcification to cardiovascular risk factors: the Multi-Ethnic study of atherosclerosis (MESA). *Atherosclerosis* **213**, 558–562. <https://doi.org/10.1016/j.atherosclerosis.2010.08.072> (2010).
5. Elmariah, S. et al. Associations of LV hypertrophy with prevalent and incident valve calcification: Multi-Ethnic study of atherosclerosis. *JACC Cardiovasc. Imaging* **5**, 781–788. <https://doi.org/10.1016/j.jcmg.2011.12.025> (2012).
6. Lee, H. J. et al. Risk factors and outcomes with progressive mitral annular calcification. *J. Am. Heart Assoc.* **12**, e030620. <https://doi.org/10.1161/JAHA.123.030620> (2023).
7. Elmariah, S. et al. Risk factors associated with the incidence and progression of mitral annulus calcification: the multi-ethnic study of atherosclerosis. *Am. Heart J.* **166**, 904–912. <https://doi.org/10.1016/j.ahj.2013.08.015> (2013).
8. Rajamannan, N. M. et al. Human aortic valve calcification is associated with an osteoblast phenotype. *Circulation* **107**, 2181–2184. <https://doi.org/10.1161/01.CIR.0000070591.21548.69> (2003).
9. Pawade, T. A., Newby, D. E. & Dweck, M. R. Calcification in aortic stenosis: the skeleton key. *J. Am. Coll. Cardiol.* **66**, 561–577. <https://doi.org/10.1016/j.jacc.2015.05.066> (2015).
10. Linefsky, J. P. et al. Association of serum phosphate levels with aortic valve sclerosis and annular calcification: the cardiovascular health study. *J. Am. Coll. Cardiol.* **58**, 291–297. <https://doi.org/10.1016/j.jacc.2010.11.073> (2011).
11. Massera, D., Kizer, J. R. & Dweck, M. R. Mechanisms of mitral annular calcification. *Trends Cardiovasc. Med.* **30**, 289–295. <https://doi.org/10.1016/j.tcm.2019.07.011> (2020).
12. Lee, J. H. et al. Reassessing the usefulness of coronary artery calcium score among varying Racial and ethnic groups by geographic locations: relevance of the Korea initiatives on coronary artery calcification registry. *J. Cardiovasc. Ultrasound* **23**, 195–203. <https://doi.org/10.4250/jcu.2015.23.4.195> (2015).
13. Lee, W. et al. Evaluation of coronary artery calcium progression in asymptomatic individuals with an initial score of zero. *Korean Circ. J.* **49**, 448–457. <https://doi.org/10.4070/kcj.2018.0318> (2019).
14. Lee, D. H. et al. The cardiovascular risk factors associated with the plaque pattern on coronary computed tomographic angiography in subjects for health check-up. *Clin. Hypertens.* **23**, 6. <https://doi.org/10.1186/s40885-017-0062-4> (2017).
15. Eberhard, M. et al. Mitral annular calcification in the elderly - Quantitative assessment. *J. Cardiovasc. Comput. Tomogr.* **15**, 161–166. <https://doi.org/10.1016/j.jcct.2020.06.001> (2021).
16. Agatston, A. S. et al. Quantification of coronary artery calcium using ultrafast computed tomography. *J. Am. Coll. Cardiol.* **15**, 827–832. [https://doi.org/10.1016/0735-1097\(90\)90282-t](https://doi.org/10.1016/0735-1097(90)90282-t) (1990).
17. Mitchell, C. et al. Guidelines for performing a comprehensive transthoracic echocardiographic examination in adults: recommendations from the American society of echocardiography. *J. Am. Soc. Echocardiogr.* **32**, 1–64. <https://doi.org/10.1016/j.echo.2018.06.004> (2019).
18. Ariza, J. et al. Peak early diastolic mitral annulus velocity by tissue doppler imaging for the assessment of left ventricular relaxation in subjects with mitral annulus calcification. *Eur. Heart J. Cardiovasc. Imaging* **17**, 804–811. <https://doi.org/10.1093/ehjci/jev219> (2016).

19. Budoff, M. J. et al. Progression of coronary artery calcium predicts all-cause mortality. *JACC Cardiovasc. Imaging*. **3**, 1229–1236. <https://doi.org/10.1016/j.jcmg.2010.08.018> (2010).
20. Fusini, L. et al. Prevalence of calcification of the mitral valve annulus in patients undergoing surgical repair of mitral valve prolapse. *Am. J. Cardiol.* **113**, 1867–1873. <https://doi.org/10.1016/j.amjcard.2014.03.013> (2014).
21. Smiseth, O. A., Baron, T., Marino, P. N., Marwick, T. H. & Flachskampf, F. A. Imaging of the left atrium: pathophysiology insights and clinical utility. *Eur. Heart J. Cardiovasc. Imaging*. **23**, 2–13. <https://doi.org/10.1093/ehjci/jeab191> (2021).
22. Nagueh, S. F. et al. Recommendations for the evaluation of left ventricular diastolic function by echocardiography: an update from the American society of echocardiography and the European association of cardiovascular imaging. *Eur. Heart J. Cardiovasc. Imaging*. **17**, 1321–1360. <https://doi.org/10.1093/ehjci/jew082> (2016).
23. Xu, B. et al. Mitral annular calcification and valvular dysfunction: multimodality imaging evaluation, grading, and management. *Eur. Heart J. Cardiovasc. Imaging*. **23**, e111–e122. <https://doi.org/10.1093/ehjci/jeab185> (2022).
24. Massera, D. et al. Disease activity in mitral annular calcification. *Circ. Cardiovasc. Imaging*. **12**, e008513. <https://doi.org/10.1161/CIRCIMAGING.118.008513> (2019).
25. Shanahan, C. M., Crouthamel, M. H., Kapustin, A. & Giachelli, C. M. Arterial calcification in chronic kidney disease: key roles for calcium and phosphate. *Circ. Res.* **109**, 697–711. <https://doi.org/10.1161/CIRCRESAHA.110.234914> (2011).
26. Li, X., Yang, H. Y. & Giachelli, C. M. Role of the sodium-dependent phosphate cotransporter, Pit-1, in vascular smooth muscle cell calcification. *Circ. Res.* **98**, 905–912. <https://doi.org/10.1161/01.RES.0000216409.20863.e7> (2006).
27. Kim, W. S., Lee, D. H. & Youn, H. J. Calcium-phosphorus product concentration is a risk factor of coronary artery disease in metabolic syndrome. *Atherosclerosis* **229**, 253–257. <https://doi.org/10.1016/j.atherosclerosis.2013.04.028> (2013).
28. Linefsky, J. P. et al. Serum phosphate is associated with aortic valve calcification in the Multi-ethnic study of atherosclerosis (MESA). *Atherosclerosis* **233**, 331–337. <https://doi.org/10.1016/j.atherosclerosis.2013.12.051> (2014).
29. Arounlangsy, P., Sawabe, M., Izumiyama, N. & Koike, M. Histopathogenesis of early-stage mitral annular calcification. *J. Med. Dent. Sci.* **51**, 35–44 (2004).
30. Bortnick, A. E. et al. Biomarkers of mineral metabolism and progression of aortic valve and mitral annular calcification: the Multi-Ethnic study of atherosclerosis. *Atherosclerosis* **285**, 79–86. <https://doi.org/10.1016/j.atherosclerosis.2019.04.215> (2019).
31. Bortnick, A. E. et al. Association of inflammatory, lipid and mineral markers with cardiac calcification in older adults. *Heart* **102**, 1826–1834. <https://doi.org/10.1136/heartjnl-2016-309404> (2016).
32. Bleyer, A. J. et al. Changes in cardiovascular calcification after parathyroidectomy in patients with ESRD. *Am. J. Kidney Dis.* **46**, 464–469. <https://doi.org/10.1053/j.ajkd.2005.04.035> (2005).
33. Ruiz-Calero, R. M., Azevedo, L. M., Bayo, M. A., Gonzales, B. & Cubero, J. J. Regression of vascular calcification in a patient with calciphylaxis. *Nephrologia* **36**, 569–571. <https://doi.org/10.1016/j.nefro.2016.03.005> (2016).
34. Seo, J. et al. Sex differences in mitral annular calcification and the clinical implications. *Front. Cardiovasc. Med.* **8**, 736040. <https://doi.org/10.3389/fcvm.2021.736040> (2021).

## Author contributions

Conceptualization, K.A.K and H.-O.J.; data curation, K.A.K and S.-Y.L.; formal analysis, K.A.K.; funding acquisition, H.-O.J.; investigation, K.A.K. and S.-Y.L.; methodology, K.A.K., H.-O.J., and H.-J.C.; project administration, H.-O.J. and H.-J.C.; resources, Y.A., M.-H.J., W.-B.C., D.-H.L., H.-O.J. and H.-J.Y.; supervision, H.-O.J.; validation, S.-Y.L. and Y.A.; visualization, K.A.K. and S.-Y.L.; writing—original draft, K.A.K.; writing—review & editing, H.-J.Y., D.H., and H.-O.J. All authors have read and agreed to the published version of the manuscript.

## Declarations

## Competing interests

The authors declare no competing interests.

## Conflict of interest

The authors declare no conflicts of interest.

## Financial support

The authors received no financial support for the research, authorship, and/or publication of this article.

## Supplementary Information

Supplementary Tables S1–S4.

Supplementary Figures S1–S4.

## Additional information

**Supplementary Information** The online version contains supplementary material available at <https://doi.org/10.1038/s41598-025-01143-7>.

**Correspondence** and requests for materials should be addressed to H.-O.J.

**Reprints and permissions information** is available at [www.nature.com/reprints](http://www.nature.com/reprints).

**Publisher's note** Springer Nature remains neutral with regard to jurisdictional claims in published maps and institutional affiliations.

**Open Access** This article is licensed under a Creative Commons Attribution-NonCommercial-NoDerivatives 4.0 International License, which permits any non-commercial use, sharing, distribution and reproduction in any medium or format, as long as you give appropriate credit to the original author(s) and the source, provide a link to the Creative Commons licence, and indicate if you modified the licensed material. You do not have permission under this licence to share adapted material derived from this article or parts of it. The images or other third party material in this article are included in the article's Creative Commons licence, unless indicated otherwise in a credit line to the material. If material is not included in the article's Creative Commons licence and your intended use is not permitted by statutory regulation or exceeds the permitted use, you will need to obtain permission directly from the copyright holder. To view a copy of this licence, visit <http://creativecommons.org/licenses/by-nc-nd/4.0/>.

© The Author(s) 2025